

Passive iFIR filters for data-driven control

Zixing Wang¹, Yongkang Huo¹, and Fulvio Forni¹

Abstract—We consider the design of a new class of passive iFIR controllers given by the parallel action of an integrator and a finite impulse response filter. iFIRs are more expressive than PID controllers but retain their features and simplicity. The paper provides a model-free data-driven design for passive iFIR controllers based on virtual reference feedback tuning. Passivity is enforced through constrained optimization (three different formulations are discussed). The proposed design does not rely on large datasets or accurate plant models.

I. INTRODUCTION

From simple prototyping to advanced control applications, a PID controller goes a long way due to its simple structure, intuitive tuning, and the presence of integral action for perfect regulation. In addition, with passive plants, PID control leads to inherently stable closed loops, even when the plant is uncertain and its model is approximated. This makes PID control one of the most common techniques in robotics and electronics [1], [2].

However, in many control applications, a stabilizing feedback action must also satisfy complex performance requirements. These are often specified as desired input/output behaviors, in the form of a set of data or a desired transfer function. In this setting, PID control shows limitations [3], [4], [5]. Ideally, we want a more flexible controller that also retains the simplicity of PID control and its fundamental properties, namely, integral action and passivity.

In this paper, we investigate the design of iFIR controllers, which combine the parallel action of a finite impulse response filter (FIR) and an integrator, for perfect regulation. Similar formulations, also based on cascade interconnections, can be found in [6], [7], [8], [9]. The idea is to replace the proportional and derivative action of the PID controller with the richer action of a FIR filter. We retain the integrator for perfect regulation. We also restrict the FIR filter to be passive, to guarantee wide applicability in the control of electro-mechanical systems and robotics [1], [2]. With integral action and passivity, our hypothesis is that iFIR controllers provide a more flexible alternative to PID control, when combined with data-driven optimal tuning.

We propose a practical design approach based on model-free data-driven methods. Passivity is enforced through constrained optimization. The data-driven design of iFIR controllers is based on virtual reference feedback tuning (VRFT) [10], which reduces the matching problem with a target

reference model to a least-squares fitting. No plant model is needed. The novelty of the paper is in endowing virtual reference feedback tuning with additional constraints for passivity. These are based on the Kalman-Yakubovich-Popov (KYP) lemma, on the Toeplitz operator of the iFIR controller, and on the positive realness of its transfer function. The result is a design approach based on convex constrained optimization, that can be solved with standard tools, such as CVX [11], [12], [13]. In what follows, we show that passivity constraints based on Toeplitz and positive realness formulations scale better with the size of the filter, strongly improving on the quadratic complexity of the KYP lemma.

When combined with passive plants, passive iFIR control leads to a neat separation between closed-loop stability and closed-loop performance. Data scarcity and low-quality data do not affect the stability of the closed loop, which is structurally guaranteed via passivity. The quality and quantity of data still matter for performance, to achieve good matching with the desired reference model. This separation between stability and performance is novel. For instance, to guarantee stability, other data-driven approaches require persistency of excitation of the probing signal [3], [14]; or provide asymptotic guarantees in the limit of infinite data length [7], [5], [15]. The idea of enforcing passivity combined to data-driven approximation is borrowed by the general kernel approach to nonlinear modeling offered by [16]. There, passivity is achieved through regularization and scattering transform. We achieve it through constrained optimization, in the narrower setting of iFIR architectures.

The paper is structured as follows. The iFIR control design based on VRFT is illustrated in Section 2. Passivity constraints are extensively discussed in Section 3. Section 4 provides an example of closed-loop control with a linear and nonlinear plants. The conclusions follow.

II. DATA-DRIVEN DESIGN OF iFIR CONTROLLERS

iFIR controllers C combine integration and finite impulse response filtering. Given the finite coefficients $\{g_k\}_{k=0,\dots,m-1}$, the controller is given by

$$C(z) = \underbrace{\frac{\gamma T_s}{1-z^{-1}}}_{\text{integrator}} + \underbrace{\sum_{k=0}^{m-1} g_k z^{-k}}_{\text{FIR part}} \quad (1)$$

where the integrator is discretized using backward Euler discretization with sampling period T_s . γ is the integral gain. Indeed, C shows a generalized PID structure, where the proportional and derivative terms are replaced by a FIR filter.

*The work of Zixing Wang was supported by CSC Cambridge Scholarship. The work of Yongkang Huo was supported by the UK Engineering and Physical Sciences Research Council (EPSRC) grant 10671447.

¹ Department of Engineering, University of Cambridge, CB2 1PZ Cambridge, UK {zwx20@cam.ac.uk, yh415@cam.ac.uk, f.forni@eng.cam.ac.uk}

C can be easily designed from data, following the approach of virtual reference feedback tuning [10]. From the block diagram in Figure 1, we represent the desired closed-loop performance with a time invariant (possibly nonlinear) reference model M_r . P is a time-invariant single-input single-output plant. The plant is not necessarily linear but we assume *passivity* from the input u to the output y . Under the action of the generic reference r , the ideal closed-loop behavior satisfies $y \simeq y^*$.

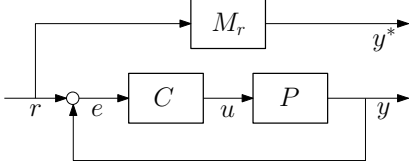


Fig. 1. Block diagram of the closed-loop system.

The controller can be derived as the solution of the following optimization problem:

$$\min_{C \in \text{iFIR}} \frac{1}{N} \sum_{t=0}^{N-1} (u(t) - C(M_r^{-1}(y) - y)(t))^2 \quad (2)$$

where $\{y(t)\}_{t=0, \dots, N-1}$ is the measured open-loop plant output when the plant is excited with a user-defined signal $\{u(t)\}_{t=0, \dots, N-1}$. The output signal y can be obtained through experiments, which makes the approach suitable to settings where a model of the plant is not fully available.

Under the ideal condition of perfect matching $y = y^*$, the idea of VRFT is to derive a compatible reference signal $r = M_r^{-1}y^* = M_r^{-1}y$, which is then used to obtain the controller C by fitting the input/output pair $(r - y, u)$. The inverse reference model M_r^{-1} is realized by a causal approximation. For linear reference models, the inverse can be removed by filtering of input and output signals via M_r itself, which leads to the filtered optimization problem

$$\min_{C \in \text{iFIR}} \frac{1}{N} \sum_{t=0}^{N-1} (M_r u(t) - C(y - M_r y)(t))^2 \quad (3)$$

Following [10], for linear plants and linear reference models, it can be shown that the minimizer of (2) also minimizes

$$\min_{C(z)} \left\| M_r(z) - \frac{P(z)C(z)}{1 + P(z)C(z)} \right\|_2^2 \quad (4)$$

if the optimal controller of the latter, $C^*(z)$, can be represented by an iFIR (1) (for $N \rightarrow \infty$ and if u is given by the realization of a stationary and ergodic stochastic process). If $C^* \notin \text{iFIR}$, pre-filtering of the open-loop data $\{u(t), y(t)\}_{t=0, \dots, N-1}$ with a suitably chosen LTI filter can reduce the difference between the two minimizers. We refer to [10] for additional details on VRFT.

Remark 1: The optimization problems in (2) and (3) are equivalent to a least-squares problem and hence can be solved efficiently. To show this, define $e = M_r^{-1}(y) - y$. Following [17, Equation 7.3], the optimization problem (2) (or (3)) with the controller (1) reads

$$\min_{g \in \mathbb{R}^m} \|u - E g + \gamma E_{\text{int}}\|_2^2 \quad (5)$$

where $g = [g_0 \ \dots \ g_{m-1}]^T$, $u = [u(0) \ \dots \ u(N-1)]^T$,

$$E = \begin{bmatrix} e(0) & 0 & \dots & \dots & 0 \\ e(1) & e(0) & 0 & \dots & 0 \\ \vdots & \vdots & & & \vdots \\ e(N-2) & e(N-3) & \dots & \dots & e(N-m-1) \\ e(N-1) & e(N-2) & \dots & \dots & e(N-m) \end{bmatrix},$$

and $E_{\text{int}} = T_s [e(0) \ e(0) + e(1) \ \dots \ \sum_{t=0}^{N-1} e(t)]^T$.

VRFT is an established and effective methodology. However, the data-driven optimal controller (2) *does not guarantee stability of the closed-loop system*. We tackle this problem via passivity.

III. PASSIVE iFIR CONTROLLERS

For passive plants P , closed-loop stability is guaranteed if the iFIR controller is passive. Hence, we combine the least-square fitting (5) with specific constraints that enforce passivity. This leads to the derivation of the passive iFIR controller that best fit the desired input/output data (2).

The first formulation is a straightforward application of Kalman-Yakubovich-Popov (KYP) lemma.

Theorem 1 (KYP approach): Given the iFIR (1) of order m , consider the state-space realization of the FIR part

$$\begin{cases} x(t+1) = Ax(t) + Bu(t) \\ y(t) = Cx_t + Du(t) \end{cases} \quad (6)$$

where $A \in \mathbb{R}^{m-1 \times m-1}$, $B \in \mathbb{R}^{m-1}$, $C \in \mathbb{R}^{m-1}$, $D \in \mathbb{R}$ are given by

$$A = \begin{bmatrix} 0 & 1 & 0 & 0 & \dots & 0 \\ 0 & 0 & 1 & 0 & \dots & 0 \\ \vdots & & & & & \\ 0 & 0 & 0 & 0 & \dots & 1 \\ 0 & 0 & 0 & \dots & & 0 \end{bmatrix}, \quad B = \begin{bmatrix} 0 \\ 0 \\ \vdots \\ 0 \\ 1 \end{bmatrix}$$

$$C = [g_{m-1} \ g_{m-2} \ \dots \ g_2 \ g_1], \quad D = g_0.$$

Define the following linear matrix inequalities

$$\gamma \geq 0 \quad (7a)$$

$$P + P^T > 0 \quad (7b)$$

$$\begin{bmatrix} P - A^T P A & \frac{1}{2} C^T - A^T P B \\ \frac{1}{2} C - B^T P A & D - B^T P B \end{bmatrix} \geq 0. \quad (7c)$$

Then, the optimal iFIR controller given by (2) and (7) is passive, thus guarantees closed-loop stability.

Proof: (7) are the standard matrix inequalities for passivity of discrete LTI systems. These are linear in the unknowns C and P . The passivity of the iFIR controller follows from the KYP lemma, recalling that the parallel interconnection of passive systems is passive. Closed-loop stability follows from the passivity theorem. ■

The attracting feature of Theorem 1 is that the constrained minimization problem can be handled efficiently by convex optimization solvers such as CVX, [11], [12], [13]. The main issue of (7) is that the number of unknowns scales as $o(m^2)$. This may cause long computation times and numerical

precision issues, leading to convergence issues when the order of the FIR part is high. The approach proposed below, overcomes these limitations.

Define the Toeplitz matrix of order $n \geq m$ associated with the coefficients $g = \{g_k\}_{k=0, \dots, m-1}$ as follows, [18]:

$$\phi_n(g) = \begin{bmatrix} g_0 & 0 & \dots & \dots & 0 \\ g_1 & g_0 & 0 & \dots & 0 \\ \vdots & \vdots & \ddots & \vdots & \vdots \\ g_{m-1} & g_{m-2} & \dots & 0 & 0 \\ 0 & g_{m-1} & \dots & g_0 & 0 \\ 0 & \dots & g_{m-1} & \dots & g_0 \end{bmatrix} \in \mathbb{R}^{n \times n}. \quad (8)$$

The first n samples of the response of the FIR filter given by g can be computed as the product between $\phi_n(g)$ and the (vectorized) input $e = [e(0), \dots, e(n-1)]^T$. It is thus not surprising that the passivity of the FIR filter is related with the positive semi-definiteness of the Toeplitz matrix $\phi_n(g) + \phi_n(g)^T$, as stated in the following theorem. In what follows the symbol $\underline{\sigma}$ denotes the minimal singular value of a matrix.

Theorem 2 (Infinite Toeplitz approach): Given the iFIR (1) of order m , let $g = \{g_k\}_{k=0, \dots, m-1}$ be the finite coefficients of its FIR part. The iFIR controller given by (2) and by

$$\gamma \geq 0 \quad (9a)$$

$$\lim_{n \rightarrow \infty} \underline{\sigma}(\phi_n^T(g) + \phi_n(g)) \geq 0 \quad (9b)$$

is passive (thus guarantees closed-loop stability).

Proof: Like the proof of Theorem 1, we just need to show that the FIR part of the filter is passive. Consider the vectorized generic input $w_n = [w_0, w_1, \dots, w_n]^T$ and associated output $z_n = [z_0, z_1, \dots, z_n]^T$ of the FIR part, where $n \geq m$. For all $n \geq m$, we have

$$z_n^T w_n = w_n^T \phi_n(g)^T w_n = w_n^T \left(\frac{\phi_n(g)^T + \phi_n(g)}{2} \right) w_n.$$

Therefore,

$$z_n^T w_n \geq 0 \quad \equiv \quad \phi_n(g)^T + \phi_n(g) \geq 0.$$

Thus, for $n \rightarrow \infty$, passivity requires (9b). ■

The main issue of Theorem 2 is that (9) is not computationally tractable. This motivates the following relaxation.

Theorem 3 (Finite Toeplitz approach): Given the iFIR (1) of order m , let $g = \{g_k\}_{k=0, \dots, m-1}$ be the finite coefficients of its FIR part. For any $\varepsilon > 0$, $\rho_0 > 0$, $0 < \rho \leq 1$, and there exists $n^* \geq m$ such that for all $n \geq n^*$, the iFIR controller given by (2) and

$$\gamma \geq 0 \quad (10a)$$

$$\rho_0 \geq |g_0| \quad (10b)$$

$$\rho_0 \rho^k \geq |g_k| \quad \forall k \in \{1, \dots, m-1\} \quad (10c)$$

$$\phi_n^T(g) + \phi_n(g) \geq \varepsilon I_n \quad (10d)$$

is passive.

Proof: Again, we just need to show the FIR part of the iFIR controller is passive.

For $n \rightarrow \infty$, the matrix $\phi_n(g)^T + \phi_n(g)$ is a $(m-1)$ -banded symmetric infinite dimensional Toeplitz matrix, [19,

Theorem 2.1], [18, pp.37]. Hence, as shown in [18, Equation 4.5] and [19, p. 322], there exists an associated generating function f given by

$$f(\omega) = g_0 + \sum_{k=-m+1}^{m-1} g_k e^{j2\pi k \omega} \quad (11)$$

where $\omega \in [-\frac{1}{2}, \frac{1}{2}]$. $\{g_k\}_{k=-\infty, \dots, \infty}$ is absolutely summable. Therefore, we can apply [18, Corollary 4.2] to obtain

$$\lim_{n \rightarrow \infty} \underline{\sigma}(\phi_n(g)^T + \phi_n(g)) = \text{ess inf}_{\omega} f(\omega) \leq \infty \quad (12)$$

where ess inf refers to essential infimum defined in [18, pp.40]. Since $|f(\omega)| \leq |g_0| + \sum_{k=-m+1}^{m-1} |g_k|$, it follows that the limit is bounded.

From the definition of limit, it follows that for any given ρ_0 , ρ , and ε satisfying the assumptions of the theorem, there exists n^* such that

$$\left| \lim_{k \rightarrow \infty} \underline{\sigma}(\phi_k^T(g) + \phi_k(g)) - \underline{\sigma}(\phi_n^T(g) + \phi_n(g)) \right| \leq \varepsilon \quad (13)$$

for all $n \geq n^*$. Thus, for any given $n \geq n^*$, (10d) guarantees $\lim_{k \rightarrow \infty} \underline{\sigma}(\phi_k^T(g) + \phi_k(g)) \geq 0$. This implies that the FIR part of the iFIR controller is passive. ■

ρ_0 , and ρ are not strictly needed for the proof of the theorem. However, these user-defined parameters determine the decay rate of the FIR coefficients, and can be used to reduce the Gibbs phenomenon due to sharp truncation of the impulse response of the FIR part of the controller. (10d) is a relaxation of (9b) based on a finite constraint plus additional bound ε . The latter reduces as n increases (and vice versa). Numerical tests show that, for large n , the Nyquist diagram of a FIR filter that satisfies $\phi_n(g)^T + \phi_n(g) \geq 0$ has a large portion of its locus on the right-half of the complex plane. To have the locus completely within the right-half plane, we can ‘shift’ the whole Nyquist diagram towards right using strictly input passivity, [20]. This is equivalent to take $\phi_n(g)^T + \phi_n(g) \geq \varepsilon I$.

Theorem 3 provides a computationally tractable optimization problem. A passive iFIR can be obtained by solving the optimization iteratively, for increasing values of n : (i) we select ρ_0 , ρ and ε and solve the optimization problem for a given $n \geq m$; (ii) we test passivity of the iFIR (from the Nyquist plot or using any other test); (iii) in case of shortage of passivity, we select a larger n (and possibly a larger ε) and iterate.

Compared with the KYP approach of Theorem 1, the finite Toeplitz approach of Theorem 2 leads to an optimization problem with $o(m)$ unknowns, linear in the order m of the iFIR filter. However, ε is not known and needs to be tuned iteratively. The following theorem overcomes this limitation. Given the coefficients $g = g_k$, in what follows we use $G(e^{j\theta})$ to denote its frequency response $\sum_{k=0}^{m-1} g_k e^{-jk\theta}$.

Theorem 4 (Positive realness approach): Given the iFIR (1) of order m , let $g = \{g_k\}_{k=0, \dots, m-1}$ be the finite coefficients of its FIR part. For any $\rho_0 > 0$, $0 < \rho \leq 1$, $M \geq 2$ the iFIR

controller by (2) and

$$\gamma \geq 0 \quad (14a)$$

$$\rho_0 \geq |g_0| \quad (14b)$$

$$\rho_0 \rho^k \geq |g_k| \quad \forall k \in \{1, \dots, m-1\} \quad (14c)$$

$$G\left(e^{\frac{iq}{M}\pi}\right) + G\left(e^{-\frac{iq}{M}\pi}\right) \geq \varepsilon \quad \forall q \in \{0, \dots, M\} \quad (14d)$$

$$\varepsilon = \pi \rho_0 \frac{1 - \rho^m}{1 - \rho} \frac{m-1}{2M} \quad (14e)$$

is passive.

Proof: We focus on the FIR part of the filter, to show that (14) implies positive realness, i.e. $G(e^{j\theta}) + G(e^{-j\theta}) \geq 0$ for all θ . The latter is equivalent to

$$\sum_{k=0}^{m-1} g_k \cos(k\theta) \geq 0 \quad \forall \theta \in [0, \pi]. \quad (15)$$

As first step, we need the following bound. Take $f(\theta) = \sum_{k=0}^{m-1} g_k \cos(k\theta)$. For all θ and Δ , we have

$$\begin{aligned} |f(\theta + \Delta) - f(\theta)| &\leq \sum_{k=0}^{m-1} |g_k| |\cos(k\theta + k\Delta) - \cos(k\theta)| \\ &\leq \sum_{k=0}^{m-1} |g_k| |k\Delta| \\ &\leq (m-1)|\Delta| \sum_{k=0}^{m-1} |g_k|. \end{aligned} \quad (16)$$

We now use (14). Let us sample f at $M+1$ points over the domain $[0, \pi]$ with a sampling interval $\frac{1}{M}$. That is, consider $f\left(\frac{q}{M}\pi\right)$ for $q \in \{0, \dots, M\}$. Then, for any given $\theta \in [0, \pi]$, find the closest sample point $\frac{q}{M}\pi$ to θ and take $\Delta = \theta - \frac{q}{M}\pi$. By construction, $-\frac{\pi}{2M} \leq \Delta \leq \frac{\pi}{2M}$ and (16) guarantees that

$$\begin{aligned} \left|f(\theta) - f\left(\frac{q}{M}\pi\right)\right| &= \left|f\left(\frac{q}{M}\pi + \Delta\right) - f\left(\frac{q}{M}\pi\right)\right| \\ &\leq (m-1)|\Delta| \sum_{k=0}^{m-1} |g_k| \\ &\leq \frac{m-1}{2M} \pi \sum_{k=0}^{m-1} |g_k| \\ &\leq \frac{m-1}{2M} \pi \rho_0 \frac{1 - \rho^m}{1 - \rho}, \end{aligned} \quad (17)$$

where the last inequality follows from (14b) and (14c), since $\sum_{k=0}^{m-1} |g_k| \leq \sum_{k=0}^{m-1} \rho_0 \rho^k$.

Thus, from (17), it is easy to see that (14d) and (14e) guarantee $G(e^{j\theta}) + G(e^{-j\theta}) = f(\theta) \geq 0$. ■

Theorem 4 follows closely [21, Section III.B] but provides the exact bound (14e), to unlock a non-iterative design of the iFIR controller. The theorem illustrates that passivity can be enforced by constraining the sampled frequency response of the FIR to be larger than a certain constant ε , which depends on the decay rate of the impulse response, the order of FIR part, and the number of sampling points in the frequency domain. This is equivalent to verify that the sampled Nyquist diagram of the FIR subcontroller has real part greater than ε . In this case, ε bounds the maximal variation of the real part of the Nyquist diagram between each two samples.

The bound (14e) is small if the ratio between the size of the FIR part, m , and the number of sampling points, M , is small. Indeed, for large orders m , this implies that either the bound ε is conservative or the optimization problem has a large number of constraints, M . The trade-off between the computational complexity and conservativeness can be mitigated by replacing the exact bound (14e) with an heuristic search over ε , based on an iteration similar to the one derived from Theorem 3.

Compared with Theorem 3, Theorem 4 leads to a one-shot design approach. In terms of complexity, Theorem 4 is more efficient than Theorems 1 and 3 since no LMIs are involved. (14d) can be implemented with $M+1$ linear inequality constraints of the form (15), for $\theta = \frac{q\pi}{M}$ and $q \in \{0, \dots, M\}$.

IV. EXAMPLES

A. Fitting of passive FIR filters

In this section we identify passive FIR filters to illustrate the effectiveness of (7), (10) and (14). Three target systems are considered:

$$C_1(s) = \frac{1}{0.5s+1} \quad C_2(s) = \frac{1}{(0.5s+1)^2} \quad C_3(s) = \frac{1}{(0.5s+1)^3}. \quad (18)$$

C_1 is passive. C_2 and C_3 show increase shortage of passivity. For each target, we take $\gamma = 0$ and we use (5) paired to passivity constraints. The input/output data (e, u) are generated as step response $u = C_i e$ for $i \in \{1, 2, 3\}$. Signals are low-pass filtered through $\frac{1}{0.2s+1}$ to improve the fitting.

Results are shown in Figure 2. The top-left plot shows that all three approaches give perfect fitting. The top-right plot shows results for conservative ε (10d). Indeed, this parameter can be used to enforce excess of passivity, to

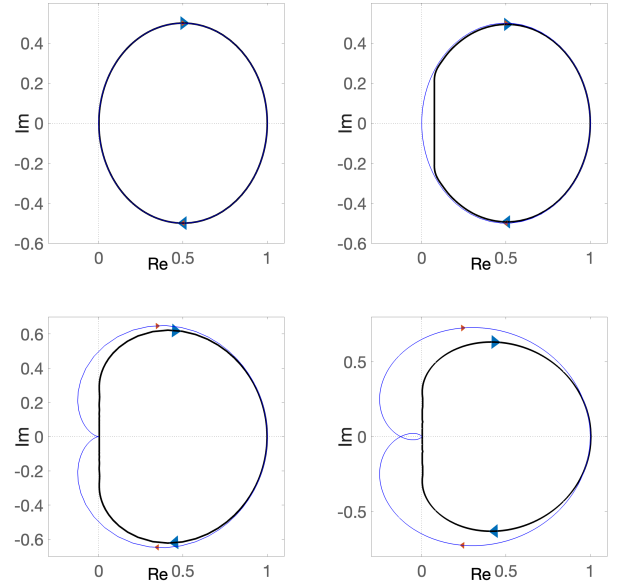


Fig. 2. Nyquist diagrams of Example IV-A. blue - target filter; black - identified passive FIR filter. Top: C_1 (left), C_1 and excess of passivity (right). Bottom: C_2 (left), C_3 (right).

compensate for shortages in the plant. Left and right bottom plots are related to the non-passive targets C_2 and C_3 . All three approaches achieve a passive FIR filter. However, as expected, the matching with the target systems degrades as the shortage of passivity increases.

B. Velocity control of a compliant mechanical system

We now develop a full iFIR controller design. Consider the two-cart plant of Figure 3, modelling a truck pulling a heavy load. The links between the truck and the load are approximated by a parallel combination of a linear spring and a linear damper. The cart masses are $m_1 = 3.0$ kg, $m_2 = 0.5$ kg. $k_{12} = 1.0$ Ns/m is the spring stiffness and $c_{12} = 1.05$ Ns/m is the damping coefficient. Each cart is also affected by additional dissipation of the form $c\dot{x}_i$, where $c = 0.5$ Ns/m and \dot{x}_i is the absolute velocity of the cart $i \in \{1, 2\}$. The block diagram for this closed-loop system is represented in Figure 1. u is the applied force and y is the velocity output.

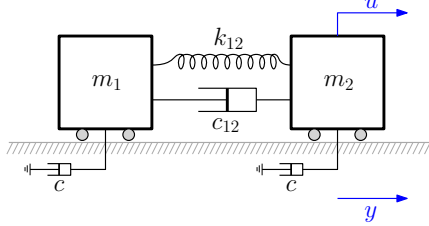


Fig. 3. A compliant two-cart system.

We consider the reference model

$$M_r(s) = \frac{1 + 0.1s}{(1 + 2\zeta sT_1 + s^2T_1^2)} \quad \zeta = 1, T_1 = 0.5.$$

The plant and the reference model are discretized with a sampling time of 0.05s. The plant is excited in open-loop with $u(t) = \sum_{i=1}^{10} \sin(\omega_i t)$ where ω_i linearly spans the frequency range of $[0.5, 10]$ rad/s, and $t \in \{0, \dots, N-1\}$. The data (e, u) for the controller are obtained as discussed in Section II and filtered with the filter $M_r(z)$.

The computation times for several iFIR controllers of order $m \in \{50, 150, 250, 350\}$ are summarized in Table I. For $m = 350$, the KYP approach takes more than one hour. This shows the advantage of (10) and (14) over (7).

	m=50	m=150	m=250	m=350
KYP	0.25 s	49.04 s	769.06 s	/
Toeplitz, $n = m$	0.07 s	0.51 s	2.81 s	4.88 s
Toeplitz, $n = 1.5m$	0.12 s	1.88 s	5.21 s	12.18 s
Toeplitz, $n = 2m$	0.17 s	3.36 s	10.62 s	61.14 s
PR, $M = m$	0.05 s	0.14 s	0.17 s	0.25 s
PR, $M = 1.5m$	0.04 s	0.14 s	0.17 s	0.24 s
PR, $M = 2m$	0.05 s	0.14 s	0.20 s	0.26 s

TABLE I

THE COMPUTATION TIMES OF CONSTRAINTS (7), (10), AND (14).

The Nyquist plots of the FIR part of the iFIR controllers are shown in Figure 4. We have taken $m = 350$, $n = 2m$ for (10) and $M = 2m$ for (14). ε is chosen heuristically. The differences between the two iFIR controllers are negligible.

On the right-part of the complex plane, both passive iFIR controllers (black) show excellent matching with the optimal unconstrained ones (blue).

The iFIR controllers are tested in simulation, as shown in Figure 5. The figure shows a comparison between iFIR controllers and the optimal PID controller $C(z) = 0.8051 + \frac{4.409T_s}{1-z^{-1}} + 0.0068 \frac{z-1}{zT_s}$. The PID gains are tuned using the VRFT approach (2). The gains are constrained to be positive for passivity. The closed-loop response of the two iFIR controllers is superior, with an almost exact matching to the target model. This is further illustrated by the Bode diagrams of the closed loop transfer functions, in Figure 7.

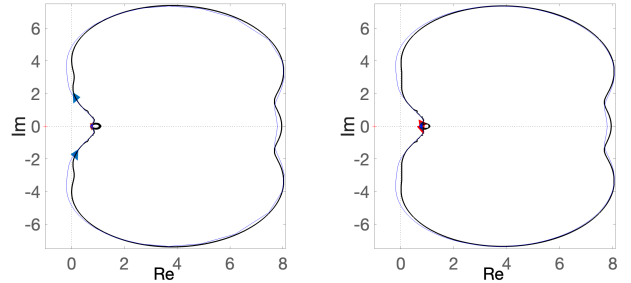


Fig. 4. Nyquist diagrams of the FIR part of the iFIR controller of Section IV-B. Left: blue - unconstrained FIR (2); black - constrained FIR (2), (10). Right: blue - unconstrained FIR (2); black - constrained FIR (2), (14).

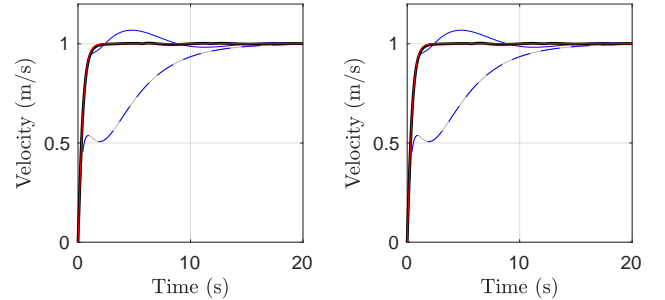


Fig. 5. Step responses. Red: target response. Black: closed-loop response with iFIR controller. Blue-continuous: closed-loop response with PID. Blue-dashed: open loop. Left plot: iFIR (2), (10). Right plot: iFIR (2), (14).

We also design and test the iFIR controller on a nonlinear passive plant. We replace the linear spring between the carts with a piece-wise linear one, as shown in Figure 6. The force-displacement characteristic has slope 1 for small displacements ($|\Delta x| \leq 0.5$) and slope 2 for large displacements ($|\Delta x| \geq 0.5$).

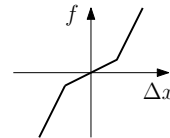


Fig. 6. Nonlinear spring.

To deal with the nonlinearity, we also reduce the aggressiveness of the reference model, by taking $T_1 = 1$. The iFIR controller is designed using (2) and (14), based on data from the nonlinear plant. Performance degrades but stability is guaranteed from passivity. The iFIR design still outperforms the optimal PID controller (based on nonlinear plant data).

V. CONCLUSIONS

We have discussed a new data-driven approach for passive iFIR controllers. Their design is based on convex optimization, combining virtual reference feedback tuning with passivity constraints. Our approach does not require any plant model nor large datasets, and the plant can be nonlinear. For passive plants, stability of the closed loop is guaranteed by

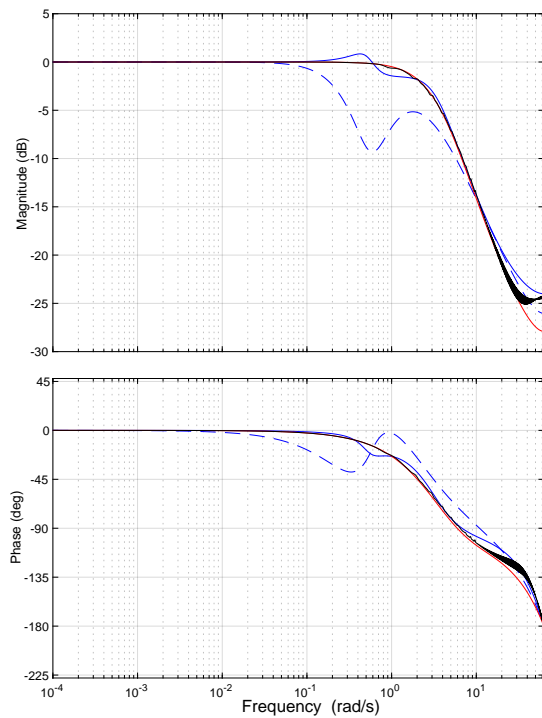


Fig. 7. Bode diagrams. Red: target reference model. Black: iFIR-based (2),(14) closed-loop transfer function from r to y Blue-continuous: PID based closed-loop transfer function. Blue-dashed: plant transfer function.

REFERENCES

- [1] M. Spong, "An historical perspective on the control of robotic manipulators," *Annual Review of Control, Robotics, and Autonomous Systems*, vol. 5, no. 1, pp. 1–31, 2022.
- [2] R. Ortega, J. Romero, P. Borja, and A. Donaire, *PID Passivity-Based Control of Nonlinear Systems with Applications*. Wiley, 2021.
- [3] A. S. Bazanella, L. Camestrini, and D. Eckhard, *Data-driven controller design: the H2 approach*. Springer Science & Business Media, 2011.
- [4] V. Bordignon and L. Camestrini, "Improving the choice of disturbance reference model in data-driven control methods," in *Congresso Brasileiro de Automática-CBA*, vol. 1, no. 1, 2019.

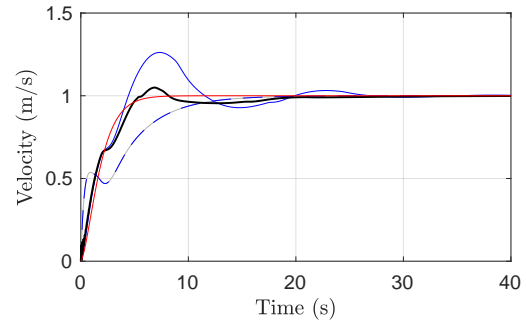


Fig. 8. Step responses of the controlled nonlinear plant. Red: target response. Black: nonlinear closed-loop response with iFIR controller. Blue-continuous: nonlinear closed-loop response with PID. Blue-dashed: nonlinear open loop.

- [5] A. Yonezawa, H. Yonezawa, S. Yahagi, and I. Kajiwara, "One-shot data-driven design of fractional-order pid controller considering closed-loop stability: fictitious reference signal approach," *arXiv preprint arXiv:2311.05869*, 2023.
- [6] S. Formentin and S. M. Savaresi, "Noniterative data-driven design of multivariable controllers," in *50th IEEE Conference on Decision and Control and European Control Conference*, 2011, pp. 5106–5111.
- [7] K. Van Heusden, A. Karimi, and D. Bonvin, "Data-driven model reference control with asymptotically guaranteed stability," *International Journal of Adaptive Control and Signal Processing*, vol. 25, no. 4, pp. 331–351, 2011.
- [8] S. Yahagi and M. Suzuki, "Direct data-driven design for a sparse feedback controller based on vrft and lasso regression," *IFAC-PapersOnLine*, vol. 55, no. 25, pp. 229–234, 2022.
- [9] T. de Jong, V. Breschi, M. Schoukens, and S. Formentin, "Data-driven model-reference control with closed-loop stability: the output-feedback case," *IEEE Control Systems Letters*, 2023.
- [10] M. C. Campi, A. Lecchini, and S. M. Savaresi, "Virtual reference feedback tuning: a direct method for the design of feedback controllers," *Automatica*, vol. 38, no. 8, pp. 1337–1346, 2002.
- [11] M. Grant and S. Boyd, "Graph implementations for nonsmooth convex programs," in *Recent Advances in Learning and Control*, ser. Lecture Notes in Control and Information Sciences, V. Blondel, S. Boyd, and H. Kimura, Eds. Springer-Verlag Limited, 2008, pp. 95–110.
- [12] —, "CVX: Matlab software for disciplined convex programming, version 2.0," <http://cvxr.com/cvx>, 2014.
- [13] S. Diamond and S. Boyd, "CVXPY: A Python-embedded modeling language for convex optimization," *Journal of Machine Learning Research*, vol. 17, no. 83, pp. 1–5, 2016.
- [14] J. Wang, S. Baldi, and H. J. van Waarde, "Necessary and sufficient conditions for data-driven model reference control," *arXiv preprint arXiv:2310.11159*, 2023.
- [15] D. Selvi, D. Piga, G. Battistelli, and A. Bemporad, "Optimal direct data-driven control with stability guarantees," *European Journal of Control*, vol. 59, pp. 175–187, 2021.
- [16] H. van Waarde and R. Sepulchre, "Kernel-based models for system analysis," *IEEE Transactions on Automatic Control*, vol. 68, no. 9, pp. 5317–5332, 2023.
- [17] G. Pillonetto, T. Chen, A. Chiuso, G. De Nicolao, and L. Ljung, *Regularized system identification: Learning dynamic models from data*. Springer Nature, 2022.
- [18] R. M. Gray *et al.*, "Toeplitz and circulant matrices: A review," *Foundations and Trends® in Communications and Information Theory*, vol. 2, no. 3, pp. 155–239, 2006.
- [19] T. Strohmer, "Four short stories about toeplitz matrix calculations," *Linear Algebra and its Applications*, vol. 343, pp. 321–344, 2002.
- [20] T. Chaffey, F. Forni, and R. Sepulchre, "Graphical nonlinear system analysis," *IEEE Transactions on Automatic Control*, 2023.
- [21] N. P. S. Prakash, Z. Chen, and R. Horowitz, "Data-driven strictly positive real system identification with prior system knowledge," in *2022 American Control Conference (ACC)*. IEEE, 2022, pp. 3949–3954.